

Photochemical & Photobiological Sciences

Accepted Manuscript



This is an *Accepted Manuscript*, which has been through the Royal Society of Chemistry peer review process and has been accepted for publication.

Accepted Manuscripts are published online shortly after acceptance, before technical editing, formatting and proof reading. Using this free service, authors can make their results available to the community, in citable form, before we publish the edited article. We will replace this *Accepted Manuscript* with the edited and formatted *Advance Article* as soon as it is available.

You can find more information about *Accepted Manuscripts* in the [Information for Authors](#).

Please note that technical editing may introduce minor changes to the text and/or graphics, which may alter content. The journal's standard [Terms & Conditions](#) and the [Ethical guidelines](#) still apply. In no event shall the Royal Society of Chemistry be held responsible for any errors or omissions in this *Accepted Manuscript* or any consequences arising from the use of any information it contains.

Photoinduced intercomponent excited-state decays in a molecular dyad made of a dinuclear rhenium(I) chromophore and a fullerene electron acceptor unit

Francesco Nastasi,^a Fausto Puntoriero,^a Mirco Natali,^b Miriam Mba,^c Michele Maggini,*^c Patrizia Mussini,^d Monica Panigati,*^{d,e} and Sebastiano Campagna.*^{a,f}*

(a) Dipartimento di Scienze Chimiche, Università di Messina and Centro Interuniversitario per la Conversione Chimica dell'Energia Solare (SOLAR-CHEM; sezione di Messina), Messina, Italy.

(b) Dipartimento di Scienze Chimiche e Farmaceutiche, Università di Ferrara and Centro Interuniversitario per la Conversione Chimica dell'Energia Solare (SOLAR-CHEM; sezione di Ferrara), Ferrara, Italy.

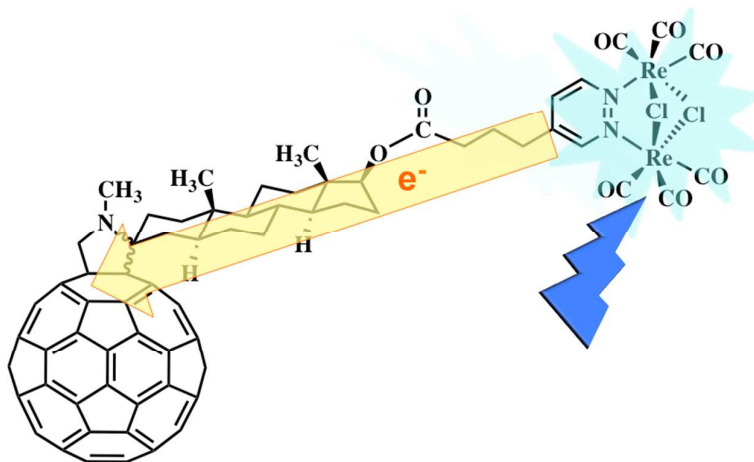
(c) Dipartimento di Scienze Chimiche, Università di Padova, Padova, Italy.

(d) Dipartimento di Chimica, Università degli Studi di Milano, Milano, Italy.

(e) Istituto per lo Studio delle Macromolecole (ISMAL)-CNR, Milano, Italy.

(f) Istituto per la Sintesi Organica e la Fotoreattività (ISOF)-CNR, Bologna, Italy.

Table of Contents Entry



The first molecular dyad, **1**, containing a pyridazine-bridged dinuclear Re(I) chromophore is prepared. A photoinduced triplet charge-separated state is formed in **1** in about 100 ps, which recombines by a spin-selective process, so forming the fullerene triplet state, within 10 ns.

ABSTRACT. A novel molecular dyad, **1**, made of a dinuclear $\{[\text{Re}_2(\mu\text{-X})_2(\text{CO})_6(\mu\text{-pyridazine})]\}$ component covalently-linked to a fullerene unit by a carbocyclic molecular bridge has been prepared and its redox, spectroscopic, and photophysical properties – including pump-probe transient absorption spectroscopy in the visible and near-infrared region - have been investigated, along with those of its model species. Photoinduced, intercomponent electron transfer occurs in **1** from the thermally-equilibrated, triplet metal/ligand-to-ligand charge-transfer ($^3\text{MLLCT}$) state of the dinuclear rhenium(I) subunit to the fullerene acceptor, with a time constant of about 100 ps. The so-formed triplet charge-separated state recombines in few nanoseconds by a spin-selective process yielding, rather than the ground state, the locally-excited, triplet fullerene state, which finally decays to the ground state by intersystem crossing in about 290 ns.

KEYWORDS - Photoinduced electron transfer; Transient absorption spectroscopy; Photoinduced charge separation; Spin-selective charge recombination; Femtosecond spectroscopy; Luminescent rhenium(I) complexes; Donor-Acceptor Compounds.

Introduction

Rhenium(I) compounds containing N-heterocyclic aromatics, like polypyridine ligands, have played key roles in the development of several fields of chemistry, such as photophysics and photochemistry,¹ photoinduced electron and energy transfer,² and photocatalysis (including CO₂ photoreduction).³ In particular, some experimental techniques, like time-resolved infrared spectroscopy, have also largely benefitted from the excited-state properties of Re(I) polypyridine complexes for their diffusion.⁴ Most of attraction of Re(I) polypyridine compounds has indeed derived from the properties of their lowest-energy level, a relatively long-lived metal-to-ligand charge transfer triplet (³MLCT) state, which (partly) deactivates by radiative process, leading to moderately intense luminescence.¹⁻⁵

In the last few years, a new family of luminescent rhenium(I) complexes have been discovered: The members of such a family are made of two {Re(CO)₃}⁺ units joined by a bridging pyridazine ligand and two ancillary anionic ligands (typically, halogens), so they can be indicated as [Re₂(μ-X)₂(CO)₆(μ-L)] (X is an ancillary anionic ligand and L is a bridging pyridazine).⁶ Like the mononuclear Re(CO)₃(LL)X complexes (where LL is a bidentate polypyridine ligand), these dinuclear species emit from ³MLCT excited states, but differently from their mononuclear counterparts, which are usually weak emitters, some of these complexes exhibit very high photoluminescence quantum yields (up to 0.5), both in deaerated solutions⁷ and in the solid state.⁸ Noteworthy, such high emission quantum yields allowed some compounds of this new family of luminophores to play the roles of emissive components in OLED^{7,8b} and of luminescent probes in biologically-relevant systems.⁹ However, detailed investigations on photoinduced electron and/or energy transfer processes involving [Re₂(μ-X)₂(CO)₆(μ-L)] species - including covalently-linked molecular dyads based on {[Re₂(μ-X)₂(CO)₆(μ-L)]} subunits - which are at the basis of any solar energy conversion scheme, have not been reported, although quite recently a member of this new

family of dinuclear Re(I) complexes has been used as a photocatalyst for CO₂ reduction.¹⁰ Also, fs pump-probe transient absorption spectra of [Re₂(μ-X)₂(CO)₆(μ-L)] species have not been studied.

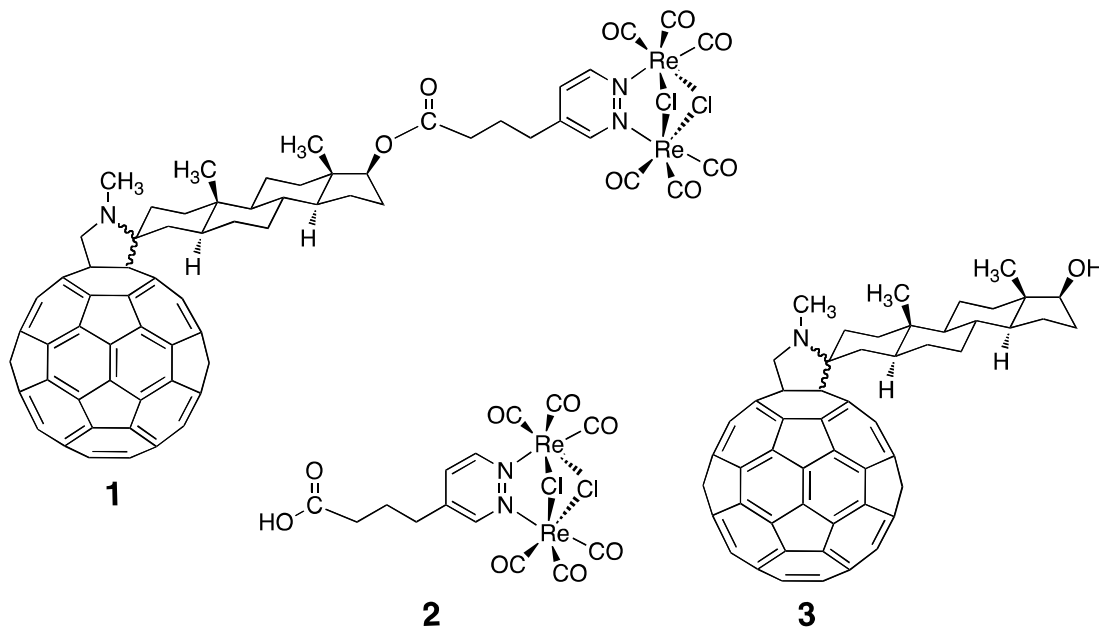


Figure 1. Structural formulae of compounds 1-3.

Here, we report on the first molecular dyad made of a [Re₂(μ-X)₂(CO)₆(μ-L)] unit covalently-linked to a fulleropyrrolidine electron acceptor (**1**, see **Figure 1**), whose synthesis is reported in the ESI. The molecular connection between the dinuclear rhenium(I) and fullerene units is provided by a short butanoate group and a rigid, non-conjugated androstane system. The absorption spectra and photophysical properties (including photoinduced intercomponent processes), studied by UV-Vis and NIR pump-probe femtosecond transient absorption spectroscopy, of **1** and of its molecular components **2** and **3** are showed and discussed. It is the first time that ultrafast transient absorption spectroscopy has been used to investigate the excited-state properties of a dirhenium compound of this new family of chromophores.

Results and Discussion

Redox behavior. The redox behavior of the family compounds of general formula $[\text{Re}_2(\mu\text{-X})_2(\text{CO})_6(\mu\text{-L})]$, to which the model species **2** belongs, have been extensively investigated.^{6-8,10} Such studies, also supported by theoretical analyses,^{6a} have demonstrated that first reduction is monoelectronic, reversible and centered on the L ligand, whereas first oxidation is usually reversible and bielectronic in nature, and involves partly delocalized orbitals receiving contributions from rhenium-centered and X-centered orbitals. Partial irreversibility of the oxidation process is found when X is chloride, probably as a consequence of the highly positive potential value induced by the presence of the strongly electron withdrawing chlorides. On the basis of this well-established framework, the already reported^{6a} redox behavior of $[\text{Re}_2(\mu\text{-Cl})_2(\text{CO})_6(\mu\text{-(4-methyl)pyridazine})]$ can be taken as a model for the redox behavior of **2**.

$\text{Re}_2(\mu\text{-Cl})_2(\text{CO})_6(\mu\text{-(4-methyl)pyridazine})]$ undergoes a quasi-reversible bielectronic oxidation at +1.67 V vs SCE in acetonitrile.⁶ The process is assigned to electrons removal from an orbital which receives contributions mainly from both rhenium(I) centers and the bridging chloride ions,^{6b} so it can be named a metal/ligand-centered orbital. The bielectronic nature of such a redox process, expected on the basis of formerly studied species of the same family, is supported by internal comparison of the intensity of the cyclic voltammetry peak corresponding to this process with that of the reduction process. Indeed, a reversible, monoelectronic reduction process takes place for $[\text{Re}_2(\mu\text{-Cl})_2(\text{CO})_6(\mu\text{-(4-methyl)pyridazine})]$ at -1.06 V, and is assigned to a pyridazine-centered orbital, in complete agreement with literature data concerning similar compounds.⁶

The cyclic voltammogram of the fullerene model compound **3**¹¹ shows a series of reversible one-electron reduction processes, the one at less negative potentials being at -0.62 V (**Table**

1). The cyclic voltammogram of **1** appears to be a combination of those of its components (see **Table 1**): in particular, oxidation involves the dinuclear “Re(μ -Cl) $_2$ Re” moiety, and the first reduction process involves the fullerene subunit. The very close redox potentials of the various subunits of **1** compared to the potential values of the corresponding redox processes of their isolated units indicate that the electronic coupling between the dinuclear rhenium and fullerene subunits is weak, as expected because of the rigidity (and lack of conjugation) provided by the aliphatic molecular bridge.

Table 1. Absorption spectra, redox and luminescence data.^a

	Absorption	Redox data		Luminescence				
	λ_{\max} [nm] (ϵ [$\text{M}^{-1}\text{cm}^{-1}$])	$E_{1/2}(\text{ox})$ V vs SCE	$E_{1/2}(\text{red})$ V vs SCE	λ_{\max} [nm] 298 K	τ [ns] 298 K	Φ 298 K	λ_{\max} [nm] 77 K	τ [μs] 77 K
1	325 (42400)	+1.67	-0.63	-	-	-	-	-
2	370 (8800)	+1.67 ^b	-1.06 ^b	575	1300 (480) ^c	0.11	503	27.6
3	325 (37000)		-0.62	715	1.3	0.001	714	0.002

[a] Absorption and luminescence data are in de-aerated toluene, unless otherwise stated; redox data of **1** are in 1,2-dichloroethane; only the potentials of first oxidation or reduction processes are reported. [b] data refers to $[\text{Re}_2(\mu\text{-Cl})_2(\text{CO})_6(\mu\text{-}(4\text{-methylpyridazine}))]$, taken as a model, in acetonitrile, see ref. 6a. [c] In parenthesis, the emission lifetime in aerated toluene solution is given.

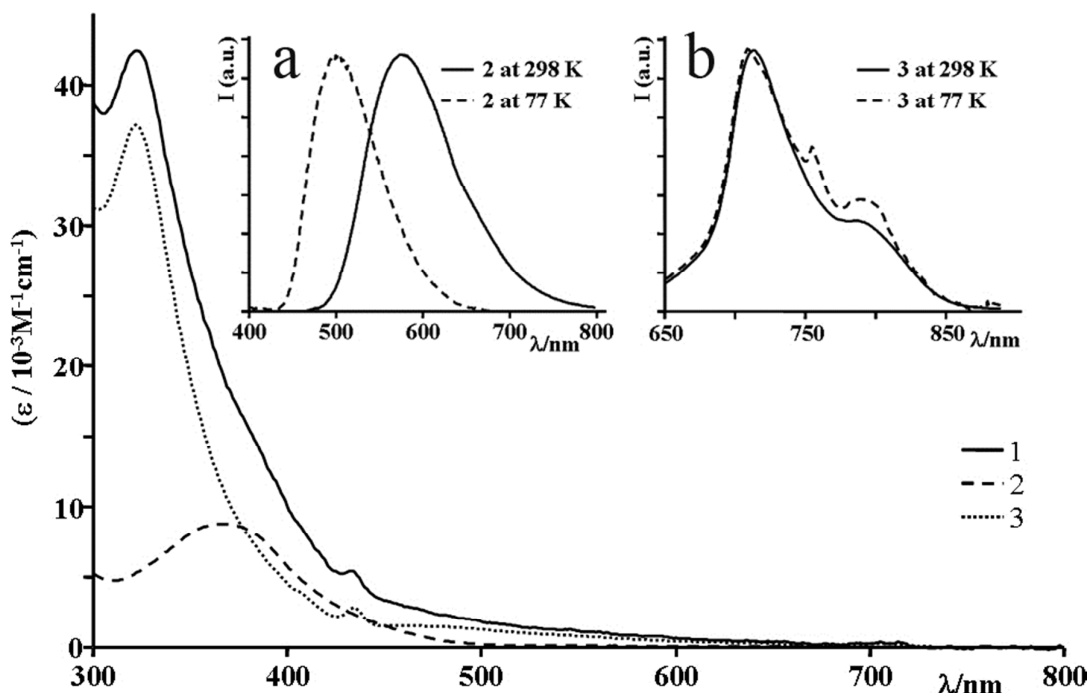


Figure 2. Absorption spectra of **1** (solid), **2** (dashed), and **3** (dotted). Inset **a** shows the emission spectra of **2** at 298 K (solid) and at 77 K (dashed). Inset **b** shows phosphorescence of **3** at 298 K (solid) and at 77 K (dashed). All spectra are in toluene; emission spectra are normalized.

Absorption spectra and photophysical properties. The absorption spectrum of **2** in toluene (**Figure 2**) is dominated by an intense absorption band with maximum at about 380 nm, assigned to a spin-allowed metal/ligand-to-ligand charge-transfer (MLLCT) transition, in agreement with the absorption spectra of other compounds of the same class of dinuclear, pyridazine-bridged Re(I) species.⁶ The band is broad, with a tail extending to 500 nm, probably containing the corresponding (less intense) spin-forbidden ³MLLCT band. The absorption band of **3** shows the usual intense absorption of fullerene species at about 320 nm. At longer wavelengths, also a small peak, typical of substituted fullerene, at about 435 nm, is present (**Figure 2**).¹² In the absorption spectrum of **1** the MLLCT band is obscured by the more intense fullerene absorption, but is clearly visible as a shoulder in the range 350 – 440 nm.

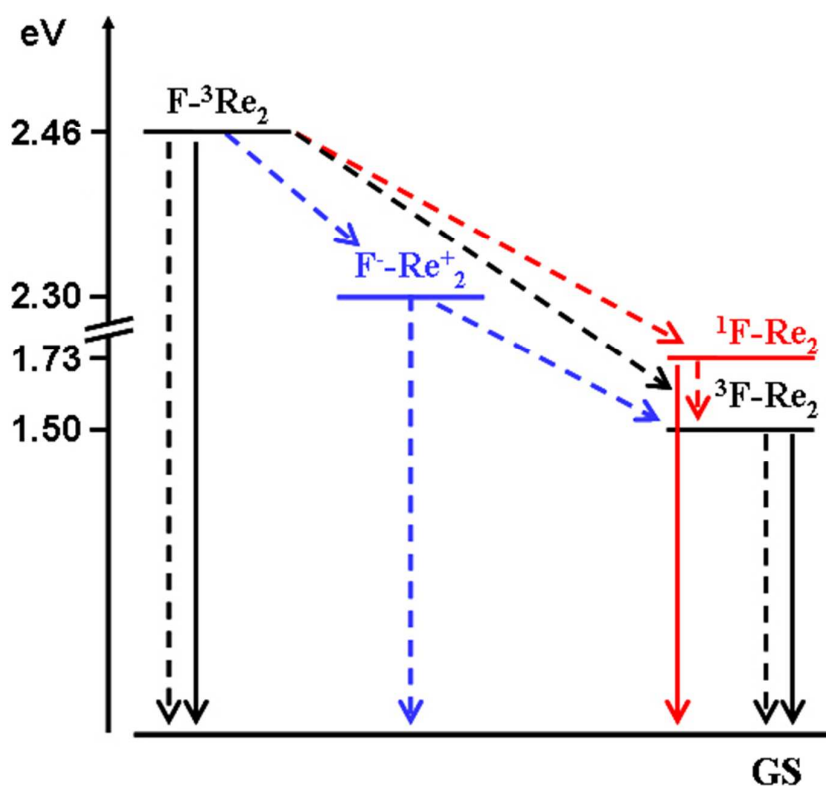


Figure 3. Excited-state energy level diagram and possible decays of **1**, indicated as F-Re₂ to evidence its bicomponent nature. Solid lines are (possible) radiative decays, and dashed ones are (possible) radiationless decays. For further details, see text.

Compound **2** is emissive in toluene, both at 77 K and at 298 K (Table 1, Figure 2, inset(a)), from its ³MLLCT state, as indicated by its emission spectra, lifetimes and quantum yield, in agreement with data of similar compounds.^{6a,9a} This emission is totally absent in **1**, indicating that new radiationless decay channels are available to the ³MLLCT state in this latter species. The energy level diagram in Figure 3, obtained on the basis of redox and luminescence data,^{†,13} shows the possible, intercomponent excited-state decay routes that are introduced in **1** by the presence of the fullerene unit: (i) electronic energy transfer to the fullerene singlet state, ¹F-Re₂ (driving force, ΔG = - 0.73 eV); (ii) electronic energy transfer to the fullerene triplet state, ³F-Re₂ (ΔG = - 0.96 eV); (iii) oxidative electron transfer to the Re₂⁺-F⁻ charge-separated state (ΔG = - 0.16 eV). Route (i) is less probable, however, since it would be spin forbidden (though the formal spin-forbidden nature of the process could be

alleviated by the presence of the heavy rhenium atom). We avoid any hypothesis of the favored quenching route based on estimation of electron or energy transfer rate constants in the light of theoretical approaches, and prefer to analyze the experimental data first, in particular the pump-probe transient absorption (TA) spectra.

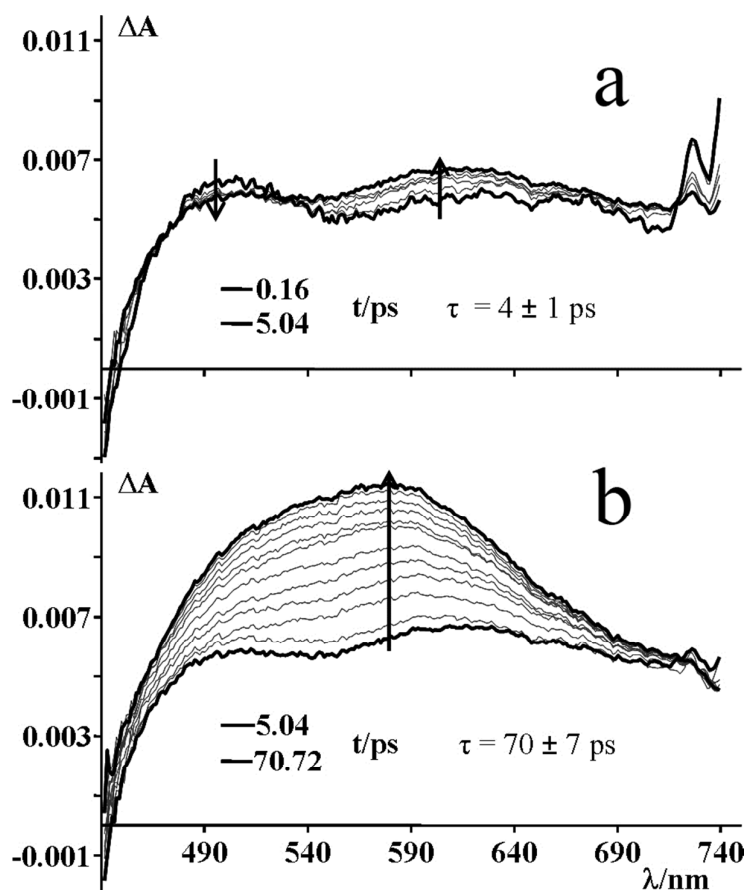
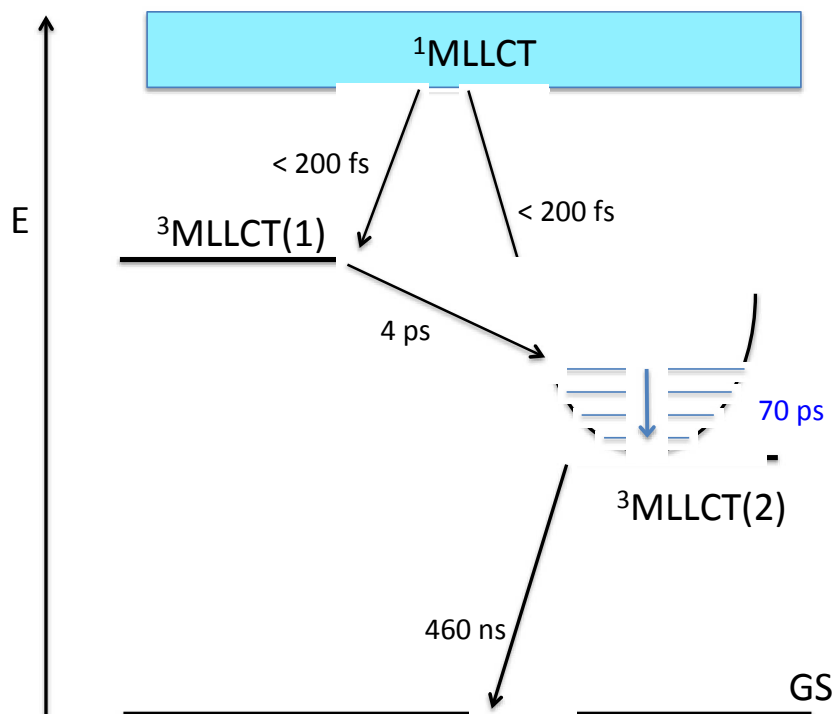


Figure 4. Transient absorption spectra of **2** in toluene (excitation wavelength, 400 nm). Time delays from pump pulse are shown in Figures (first and last delays are reported for each panel). For more details, see text.

To study the excited-state decay route of **1**, pump-probe transient absorption spectra were performed, starting with the component **2**, whose time-resolved TA spectra in toluene is shown in **Figure 4**: the initial spectrum (160 fs after laser pulse; excitation wavelength, 400 nm) exhibits two clearly discernable absorption bands in the visible region and suggests that

a bleach, assigned to disappearance of the MLLCT band, appears at shorter wavelengths than 460 nm (not shown; for technical reasons, we cannot obtain TA spectra with acceptable signal-to-noise ratio at wavelengths shorter than 450 nm). Within a few ps (time constant of the process, measured at 590 nm, $4 (\pm 1)$ ps; see **Figure 4a**) the absorption around 490 nm decreases and the one in the 540 - 670 nm range increases. On a longer timescale, the spectrum continues to evolve, until a stronger absorption, peaking at about 580 nm, is fully developed (**Figure 4b**; time constant of this process, $70 (\pm 7)$ ps). Successively, the TA spectrum monotonically decays to zero. This process, not accessible to our fs apparatus, has been checked on the ns timescale by following the recovering of the MLLCT bleach at 400 nm (excitation, 355 nm) with a ns flash photolysis equipment, see **Figure S1** in ESI. The time constant of this latter process, 461 ns, very well agrees with the emission decay of **2** (480 ns, see **Table 1**). Although it is the first time that time-resolved TA spectroscopy of a member of the family of $[\text{Re}_2(\mu\text{-X})_2(\text{CO})_6(\mu\text{-L})]$ luminophores is disclosed, so it cannot be compared to existing cases, the interpretation of the reported time-resolved processes can however be made on the basis of the literature data accumulated on mononuclear Re(I) polypyridine compounds: the "initial" spectrum of **2** here recorded (after 160 fs from pump pulse) is attributed to the triplet MLLCT manifold, since intersystem crossing in MLCT states of tricarbonyl Re(I) polypyridine compounds have been reported to occur in times shorter than 150 fs,¹⁴ therefore we assume that it occurs on a similar timescale in the present dirhenium chromophores. In mononuclear $[\text{Re}(\text{CO})_3(\text{LL})\text{Y}]^n$ species (Y = Cl, n = 0; Y = pyridine derivatives, n = 1+), however, time-resolved infrared spectroscopy indicates that two triplet states are populated simultaneously from the initially prepared singlet state, which successively equilibrate within few picoseconds.¹⁴ By analogy, the 7 ps process showed in **Figure 4a** is tentatively assigned to equilibration between slightly different MLLCT triplets. Solvent relaxation would be involved in the 70 ps process (**Figure 4b**), which finally leads to

the thermally-equilibrated, long-lived and emissive $^3\text{MLLCT}$ level.^{14b} **Scheme 1** schematizes the excited states and decays occurring in **2**. An important information that can therefore be derived by the present results is that the early events of excited state decay of the dirhenium(I) compounds, here represented by **2**, are qualitatively very similar to the early events occurring in mononuclear Re(I) polypyridine compounds.



Scheme 1. Excited state diagram (not scaled) and kinetics involved in the deactivation of the model species **2**. $^1\text{MLLCT}$ identifies the upper-energy excited states initially populated by light excitation and eventually decayed to the lowest-energy singlet state. $^3\text{MLLCT}(1)$ and $^3\text{MLLCT}(2)$ states are the two different triplet CT states populated via intersystem crossing (see text and also ref. 14). Vibrational cooling within the $^3\text{MLLCT}$ state is indicated by the blue arrow, for simplicity, also vibrational levels within this state are indicated in blue, to differentiate them from the electronic states, indicated in black. Energy potential curve is only showed for the lowest-energy CT state, where vibrational cooling is comparatively slow with respect to decays among higher-energy electronic states. GS is the ground state. This interpretation is inspired by a similar interpretation used for the excited-state decay of mononuclear Re(I) compounds.¹⁴

With the information gained from the TA spectroscopy of **2**, we can analyze the time-resolved TA spectra of **1**, shown in **Figure 5**. Four successive processes can be identified, starting from the initially-recorded spectrum. The first two processes (see **Figure 5a**), are qualitatively similar to those of **2**, with (i) the first one showing a decrease in the absorption at about 490 nm and an increase of the transient absorption in the 550 – 640 nm region (time constant, 4 ± 1 ps) and (ii) the second one in which the transient absorption in the 460 – 670 nm range increases (time constant, 20 ± 2 ps). Comparison between spectral changes and time constants of TA data of **1** and **2** suggests that (i) and (ii) processes in **1** have the same origin than the first two processes in **2**, that is reorganization processes within the dirhenium-based, triplet manifold(s), leading to the thermally-equilibrated $^3\text{MLLCT}$ state. Successively, the TA of **1** decays without any significant change (process (iii), time constant 120 ± 27 ps, see **Figure 5b**), then process (iv) occurs, revealed by a spectral profile change, with a strong decrease of the absorption in the region 450 – 650 nm and a concomitant appearance of an absorption maximum at about 695 nm (**Figure 5c**); the process is too slow to our fs apparatus, which only allowed to estimate a limit for the time constant (i.e., longer than 3 ns). To analyze the slow process we performed ns flash photolysis, which indicated that the final TA spectrum recorded by the fs apparatus corresponds to that recorded after 50 ns (**Figure S2 in ESI**), and is quite similar to that reported for triplet states of other fullerene compounds,^{12,15} so it is assigned to the triplet state of the fullerene unit, which finally decays to the ground state with a time constant of 286 ns (**Figure S2**).[#] Such a decay is short for a fullerene intersystem crossing, usually occurring in the microsecond timescale, however is probably accelerated by enhanced spin-orbit coupling induced by the presence of the two rhenium atoms.

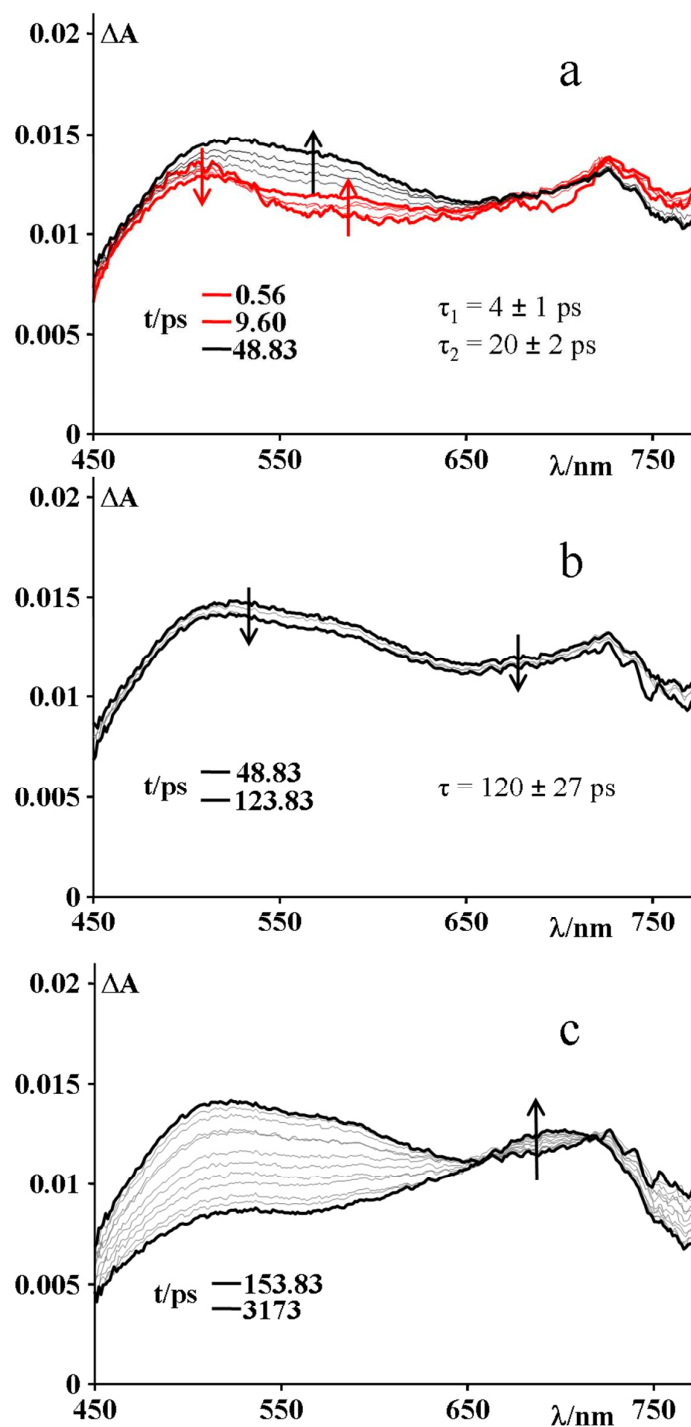


Figure 5. Transient absorption spectra of **1** in toluene (excitation wavelength, 400 nm). Time delays from pump pulse are shown in Figures (first and last for each panel, except for b, which shows three spectra, identified by colors and arrows). For details, see text.

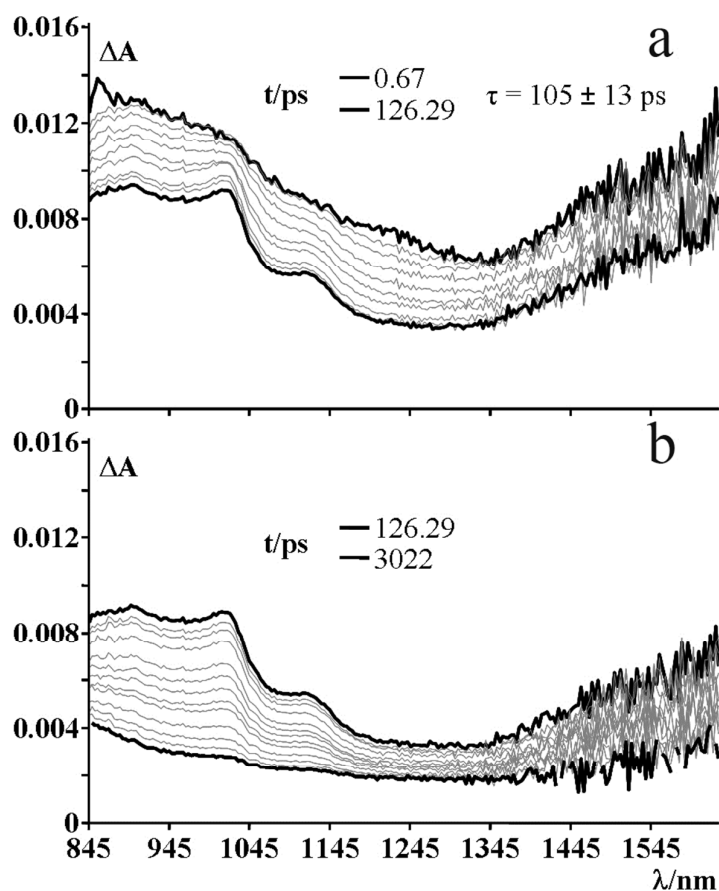


Figure 6. NIR transient absorption spectra of **1**. Time delays from pump pulse are shown in Figures (first and last for each panel; transient absorption spectra intensity is decreasing with time at any wavelength). For more details, see text.

To better study the processes (iii) and (iv), the near-infrared (NIR) spectral region (845 – 1600 nm) has been investigated. For compound **2**, TA spectroscopy in the NIR did not give any sizeable signal (see ESI, **Figure S3**). On the contrary, a broad absorption appears in the initially-recorded (600 fs after laser pulse) TA spectrum of **1** in the 850 – 1250 nm region (**Figure 6**). This TA decreases at any wavelengths, but spectral changes occur, with the appearance of a structure peaking at about 870, 1020 and 1130 nm (**Figure 6, top panel**). Such a spectral evolution takes place with a time constant of 105 (\pm 13) ps, and therefore is attributed to the process (iii), occurring in the same time range, shown in **Figure 5b**. Spectroelectrochemical study indicates that the reduced anion of **3** (that is, the fullerene

anion) has similar signatures (see **ESI**, Figure S4),¹⁶ so process (iii) is suggested to be photoinduced oxidative electron transfer from the thermally-equilibrated ³MLLCT state of the dirhenium subunit to the fullerene acceptor, with formation of the Re₂⁺-F⁻ charge-separated state (CS). Rate constant of the photoinduced charge separation process originating from the ³MLLCT state is therefore about $9.5 \times 10^9 \text{ s}^{-1}$ in **1**. The successive disappearance of the structured absorption in the NIR (**Figure 6**, bottom panel) takes place with similar time constant of process (iv) in **Figure 5** (that is, in the range 3-10 ns, see also note #), so it can be attributed to population of the triplet fullerene-centered state from the CS state. In fact, triplet excited states of fullerene derivatives have been reported to exhibit an absorption peak in the range 675 – 705 nm,^{15,17} similar to that shown in **Figure 5c**, and formed by process (iv) described above.

On the basis of the above discussion, the general main scheme for the excited state decay of **1** can be represented as in **Figure 7**. Further comments can be added, based on the experimental data. First of all, part of the exciting light at 400 nm is directly absorbed by the fullerene subunit (see absorption spectra in **Figure 2**). However, fluorescence of fullerene does not take place, so indicating that fast radiationless decay processes also deactivate such fullerene-based singlet excited state. Most likely it is a fast intersystem crossing to fullerene triplet state, accelerated by the presence of the heavy dirhenium subunit to be responsible for fullerene fluorescence quenching. Actually, the effect of the dirhenium subunit in accelerating spin-orbit coupling in the fullerene subunit in **1** is also evident in the already-mentioned, relatively short fullerene triplet lifetime, 286 ns, see above. Spectroscopic signatures of excited-state decay process emanating from the fullerene singlet state are probably buried within the larger spectroscopic changes derived from the dirhenium-based, MLLCT excitation (in particular, the broad transient absorption growing up in the visible on the timescale of tens of ps, see **Figures 4b** and **5a**).

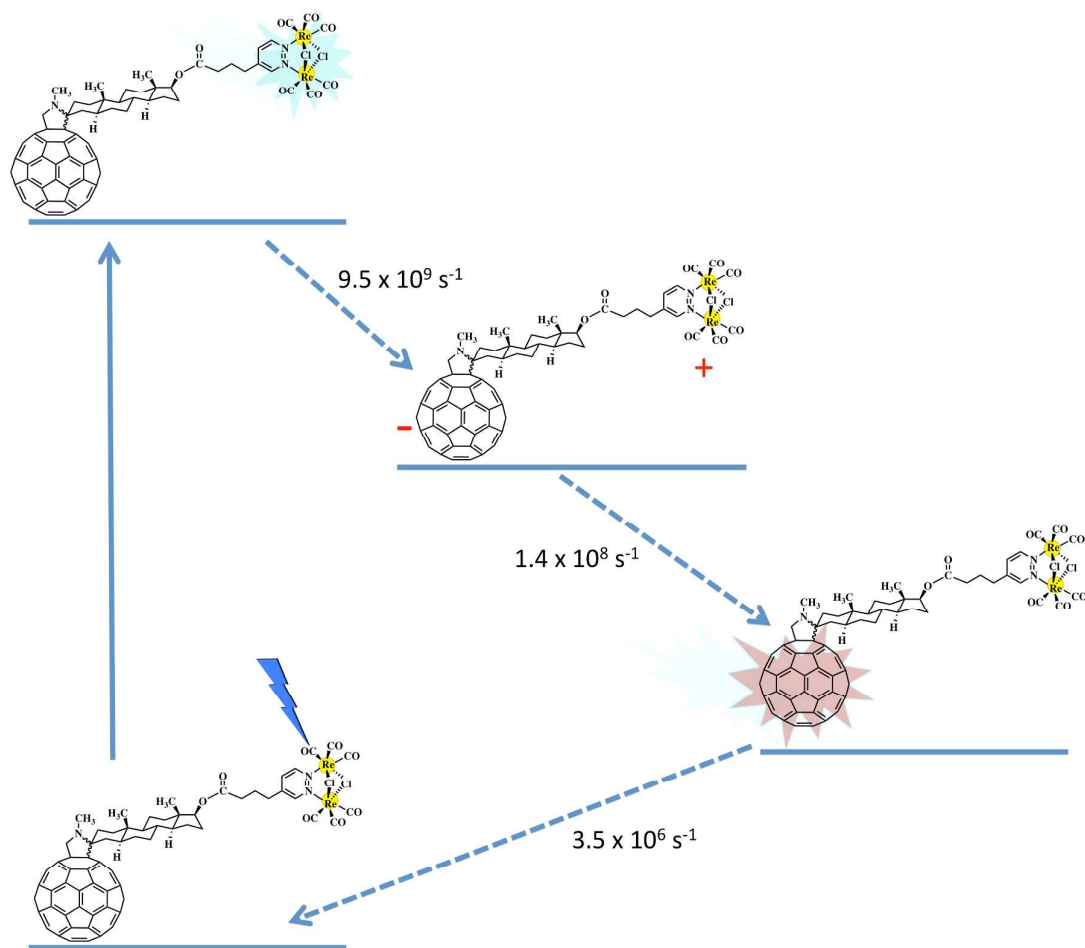


Figure 7. Schematic representation of the main excited-state decay route following $^3\text{MLLCT}$ state formation of **1**, at room temperature in fluid solution. All the states (except the ground state) are triplets. State diagrams is not in scale. The rate constant for the formation of the triplet fullerene state from the CS state has been calculated by assuming an average value for the time constant limits of this processes (3 and 10 ns), as estimated by fs pump-probe and ns flash photolysis experiments). For details, see text.

As a further confirmation of the occurring of photoinduced electron transfer as the main decay of the MLLCT triplet state of **1** at room temperature, it can be noted that spin-forbidden energy transfer from the $^3\text{MLLCT}$ state to the fullerene singlet state via Coulombic mechanism can be estimated by the simplified Förster equation (see details in ESI).^{5a} Even for quite compact structural arrangements of **1**, with edge-to-edge donor-acceptor distance as close as 10 Å (smaller than the size of the steroid moiety of the spacer), time constant for

Förster energy transfer is not smaller than 10 ns, therefore the Coulombic energy transfer cannot compete with the charge separation process, which is about two orders of magnitude faster (ca. 100 ps, from experimental data). Estimation of Dexter, electron-exchange energy transfer rate constant, which could contribute to the $^3\text{MLLCT}$ quenching and could also involve the fullerene triplet state as the acceptor, is not made in detail. The time-resolved TA spectroscopy experiments, anyway, indicate that charge separation dominates, at least at room temperature, although Dexter energy transfer to the fullerene triplet state would have a much higher driving force (-0.96 eV) than electron transfer (-0.16 eV; see above and also **Figure 3**). Since $^3\text{MLLCT}$ quenching is also present at 77 K in rigid matrix, where electron transfer are usually much slower, except in favored cases (i.e., for activationless electron transfer processes; Dexter energy transfer can also be slowed down on passing to lower temperature, but to a smaller extent than electron transfer processes), we cannot exclude that Dexter energy transfer becomes the dominant contribution to the $^3\text{MLLCT}$ decay on passing from room temperature fluid solution to 77 K rigid matrix.

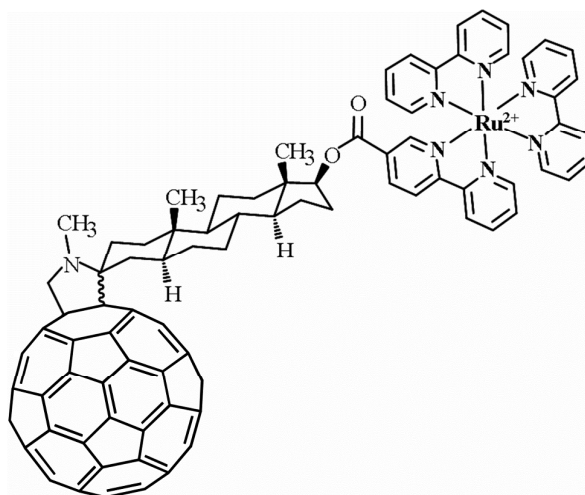


Figure 8. Structural formula of the molecular dyad **4**,¹⁷ similar to compound **1**. Charge of the compound is omitted.

Comparison with molecular analogues. It is interesting to compare the results here obtained for the new molecular dyad **1** with the properties of similar molecular dyads containing fullerene units as the acceptor and other metal-based complexes as donors. Indeed, D-fullerene dyads in which D is a Ru(II) polypyridine unit,^{11,17,18} an Ir(III) cyclometalated chromophore,¹⁹ a dinuclear Cu(I) helicate chromophore,²⁰ or a mononuclear Re(I) polypyridine unit²¹ have been reported. In most cases, the ³MLCT excited state is quenched by oxidative electron transfer processes similar to that found for **1**, so generating charge-separated states containing a reduced fullerene subunit. Probably the most relevant species, with respect to the system here studied, is the compound **4**, whose molecular structure is shown in **Figure 8**.¹⁷ This latter D-A species contains a very similar spacer, differing from **1** only for the absence of a flexible alkyl chain connecting the steroid subunit of the spacer to the metal-based chromophore. In **4**, the ³MLCT state is quenched by electron transfer to fullerene with time constants of about 1.4 ns in a toluene/CH₂Cl₂ mixture, 470 ps in CH₂Cl₂, and 196 ps in acetonitrile.¹⁷ Differences in electron transfer rates have been attributed to the solvent polarity effect, in particular to the different stabilization of the CS state occurring in more polar solvents (i.e., acetonitrile), making the electron transfer more favorable from a thermodynamic viewpoint. Interestingly, in acetonitrile the charge-separated state formed in **4** decays to the ground state through the energetically lower-lying triplet excited state involving the fullerene subunit (the triplet fullerene level is estimated to be 0.23 eV lower than the CS state in this solvent), that is *via* a spin-selective recombination process, analogously to what happens in **1**, whereas in CH₂Cl₂ the CS state undergoes excited-state equilibration with the ³MLCT Ru-based level, whose energy is very close to that of the CS state in such solvent (energy difference between the two states has been calculated to be 0.02 eV, compatible with excited-state equilibration).¹⁷ In the case of **1**, the photoinduced charge separation is formed with a time constant of about 110 ps. Considering the driving force of

the same process of **4** calculated in acetonitrile (-0.24 eV),¹⁷ the driving force estimated for **1** in toluene (-0.16 eV), and the different nature of the two solvents (driving force would favor **4**, but "costs" in terms of reorganization energy would favor **1**, since outer reorganization energy for CS is expected to be lower in less polar solvents), the difference in time constants of the photoinduced charge separation process in the two cases is acceptable. Excited-state equilibration is also fully excluded in **1** in toluene, since such a situation should allow for ³MLLCT emission from the dirhenium-based chromophore to be detected, although with a reduced quantum yield with respect to the model species **2**, and this is not the case for **1**.

Noteworthy, photoinduced, oxidative charge separation followed by recombination via the fullerene triplet state analogous to the excited-state decay route found for **1** is also reported to occur for an Ir(III) cyclometalated / fullerene system, where phosphorescence of the fullerene triplet at 77 K also takes place.¹⁹

Conclusions

In conclusion, we have synthesized the first molecular dyad, **1**, containing the dinuclear rhenium(I) $\{[\text{Re}_2(\mu\text{-X})_2(\text{CO})_6(\mu\text{-pyridazine})]\}$ moiety as the chromophore subunit. Compound **1** does not exhibit any emission, since the strongly emissive metal/ligand-to-ligand charge-transfer (³MLLCT) state of its chromophoric subunit is efficiently quenched, via oxidative electron transfer, by the (covalently-linked) fullerene subunit. The intercomponent, photoinduced electron transfer processes occurring in **1** have been studied in some detail by pump-probe femtosecond absorption spectroscopy, both in the visible and in the near infrared region. By the way, it is also the first time that such a technique is employed to investigate the excited-state properties of a member of this dinuclear class of rhenium complexes. The charge-separated (CS) species $\text{Re}_2^+\text{-F}^-$ is formed from the thermally-equilibrated ³MLLCT excited state of the dirhenium subunit by electron transfer to the

fullerene acceptor unit, with a time constant of about 110 ps. Because of the triplet nature of the MLLCT state, the so-formed CS is also expected to be a triplet state. Such a CS species decays, with a time constant of few ns, to the fullerene triplet state. Successive charge recombination is spin selective, *i.e.*, the triplet CS state recombines to yield, rather than the ground state, a locally-excited (fullerene-centered) triplet state. Beside spin reasons, even thermodynamics can favor charge recombination (CR) to the triplet fullerene state over CR to the ground state. In fact, driving force for CR to the triplet fullerene state is about 0.80 eV, whereas CR to the ground state is about 2.30 eV, so this latter process could well be within the Marcus inverted region and definitely slower than the former one. The fullerene triplet excited state finally decays to the ground state by intersystem crossing on the hundreds of nanoseconds timescale.

Although the lifetime of the CS of **1** is limited owing to the presence of the triplet fullerene state, it is still much faster than charge separation rate constant and promises to be long-lived enough to allow stepwise injection of the electron transiently stored on the fullerene framework into another, better electron acceptor substrate, for example other carbon nanostructures, eventually connected to the fullerene subunit. This would produce triads with long-lived fully-developed CS states. Work towards this direction is planned in our laboratories.

Acknowledgments

The authors thank MIUR (FIRB Project *Nanosolar*, RBAP11C58Y, PRIN Project *Hi-Phuture*, 2010N3T9M4, and PRIN Project 2009PRAM8L) and Cost Action 1202 *PERSPECT H2O* for funding and Michele Cristofani (University of Padova) for working out detailed experimental procedures.

NOTES AND REFERENCES

- (a) *Dipartimento di Scienze Chimiche, Università di Messina and Centro Interuniversitario per la Conversione Chimica dell'Energia Solare (SOLAR-CHEM; sezione di Messina), Messina, Italy.*
- (b) *Dipartimento di Scienze Chimica e Farmaceutiche, Università di Ferrara and Centro Interuniversitario per la Conversione Chimica dell'Energia Solare (SOLAR-CHEM; sezione di Ferrara), Ferrara, Italy.*
- (c) *Dipartimento di Scienze Chimiche, Università di Padova, Padova, Italy.*
- (d) *Dipartimento di Chimica, Università degli Studi di Milano, Milano, Italy.*
- (e) *Istituto per la Sintesi Organica e la Fotoreattività (ISOF)-CNR, Bologna, Italy.*

Electronic Supplementary Information (ESI) available: General procedures, equipments and methods; synthesis and characterization details; ns flash photolysis of **1** and **2**; near-infrared fs transient spectrum of **2**; global kinetic analysis of **1**, comments on the possible presence of diastereoisomers in **1**, spectroelectrochemistry of **3**.

¥ The assignment of the 70 ps component in the excited-state decay of **2** to solvent relaxation could seem surprising, since vibrational cooling, including solvent relaxation, in metal polypyridine complexes commonly takes place with time constants smaller than 10 ps. However, slow local solvent-restructuring processes (in the range 15-40 ps, with a compound also exhibiting an excited-state decay with a component longer than 70 ps) have been recently assumed to explain excited-state decay components in some mononuclear Re(I) compounds containing polypyridine and carbonyl ligands.^{14c} Our interpretation here is presented to fit into the suggested figure. To discuss the origin of the slowness of the solvent relaxation process in such compounds it is speculative at this stage, we can only offer the hypothesis that the fact that carbonyls are strongly involved in the excited-state of **2** (and probably of the mononuclear compounds discussed in ref. 14b), coupled with the fact that carbonyls can strongly interact with solvent, may have a role.

† The energy of the states indicated as $F\text{-}^3\text{Re}_2$ and $^1\text{F-Re}_2$ in Figure 3 are approximated to the 77 K emission of **2** and **3**, respectively. The energy of the $^3\text{F-Re}_2$ state is approximated to

the triplet state energy of C₆₀, and finally the energies of the charge-separated state, F⁻-Re₂⁺, is obtained by calculating the driving force for the photoinduced oxidative electron transfer process from *Re₂ to the fullerene unit, ΔG, using the simplified equation $\Delta G = e(E_{\text{ox}} - E_{\text{red}}) - E^{00}$, where E_{ox} is the ground state oxidation potential of the donor chromophore, E_{red} is the reduction potential of the acceptor (both expressed in V), E⁰⁰ is the excited state energy of the donor (in eV), assumed as the emission maximum of its model **2** at 77 K. The term *e* is the electron charge.¹³ In this equation, the work term is neglected. It can be noted, anyway, that spectroscopic and redox data have been obtained in different solvents because of technical problems (see Table 1), so the calculated values should be considered with some care.

A risetime is present in the ns flash photolysis experiment (see ESI, Fig. S2). This risetime, which should include the process (iv) cited above as the rate limiting step, is too fast to be fitted by our flash photolysis apparatus. This, however, allows to identify a time limit for the process (iv), that together with the limit identified by fs spectroscopy, indicates that the process leading to the triplet state of the fullerene subunit in **1** occurs with a time constant between 3 and 10 ns.

- (1) The literature on this topic is too vast to be exhaustively quoted. For some examples, see the following papers and the ones in refs. 2 and 3. (a) J. V. Caspar and T. J. Meyer, Application of the Energy Gap Law to Nonradiative, Excited-State Decay. *J. Phys. Chem.*, 1983, **87**, 952–957. (b) A. Juris, S. Campagna, I. Bidd, J.-M. Lehn and R. Ziessel, R. Synthesis and Photophysical and Electrochemical Properties of New Halotricarbonyl(polypyridine)rhenium(I) Complexes. *Inorg. Chem.*, 1988, **27**, 4007-4011. (c) H.Kunkely and A. Vogler, Excited State Properties of Organometallic Compounds of Rhenium in High and Low Oxidation States, *Coord. Chem. Rev.*, 2000, **200-202**, 991-1008. (d) J. G. Vaughan, B. L. Reid, S. Ramchandani, P. J. Wright, S. Muzzioli, B. W. Skelton, P. Raiteri, D. H. Brown, S. Stagni and M. Massi, The Photochemistry of Rhenium(I) Tricarbonyl N-heterocyclic Carbene Complexes. *Dalton Trans.*, 2013, **42**, 14100-14114. (e) A. Kumar, S.-S. Sun and A. J. Lees, Photophysics and Photochemistry of Organometallic Rhenium Diimine Complexes. *Top. Organomet. Chem.*, 2010, **29**, 1-35. (f) R. Kirgan, B. P. Sullivan and D. P. Rillema, Photochemistry

- and Photophysics of Coordination Compounds: Rhenium. *Top. Curr. Chem.*, 2007, **281**, 45-100.
- (2) T. J. Meyer, Photochemistry of Metal Coordination Complexes: Metal to Ligand Charge Transfer Excited States. *Pure Appl. Chem.*, 1986, **58**, 1193-1206. (b) G. Tapolsky, R. Duesing and T. J. Meyer, Synthetic Control of Excited-State Properties in Ligand-Bridged Complexes of Rhenium(I). Intramolecular Energy Transfer by an Electron-Transfer/Energy-Transfer Cascade. *Inorg. Chem.*, 1990, **29**, 2285-2297. (c) K. S. Schanze, D. B. MacQueen, T. A. Perkins and L. A. Cabana, Studies of Intramolecular Electron and Energy Transfer Using the fac-(diimine)Re^I(CO)₃ Chromophore. *Coord. Chem. Rev.*, 1993, **122**, 63. (d) Y. Yue, T. Grusenmeyer, Z. Ma, P. Zhang, R. H. Schmehl, D. N. Beratan and I. V. Rubtsov, Full-Electron Ligand-to-Ligand Charge Transfer in a Compact Re(I) Complex. *J. Phys. Chem. A*, 2014, DOI: 10.1021/jp5039877. (e) T. Asatani, Y. Nakagawa, Y. Funada, S. Sawa, H. Takeda, T. Morimoto, K. Koike and O. Ishitani, Ring-Shaped Rhenium(I) Multinuclear Complexes: Improved Synthesis and Photoinduced Multielectron Accumulation. *Inorg. Chem.*, 2014, **53**, 7170-7180.
- (3) (a) J. Hawecker, J.-M. Lehn and R. Ziessel, Photochemical and Electrochemical Reduction of Carbon Dioxide to Carbon Monoxide Mediated by (2,2'-Bipyridine) tricarbonylchlororhenium(I) and Related Complexes as Homogeneous Catalysts. *Helv. Chim. Acta* 1986, **69**, 1990-2012. (b) E. Fujita, Photochemical Carbon Dioxide Reduction with Metal Complexes, *Coord. Chem. Rev.*, 1999, **185-186**, 373-384. (c) H. Takeda, K. Koike, H. Inoue and O. Ishitani, Development of an Efficient Photocatalytic System for CO₂ Reduction Using Rhenium(I) Complexes Based on Mechanistic Studies, *J. Am. Chem. Soc.*, 2008, **130**, 2023-2031. (d) E. Portenkirchner, K. Oppelt, D. A. M. Egbe, G. Knör and N. S. Sariçiftçi, Electro- and Photo-chemistry of Rhenium and Rhodium Complexes for Carbon Dioxide and Proton Reduction: a Mini Review, *Nanomaterials and Energy*, 2013, **2**, 134-147. (e) T. Morimoto, T. Nakajima, S. Sawa, R. Nakanishi, D. Imori and O. Ishitani, CO₂ Capture by a Rhenium(I) Complex with the Aid of Triethanolamine, *J. Am. Chem. Soc.*, 2013, **135**, 16825-16828.
- (4) (a) J. R. Schoonover, G. F. Strouse, B. D. Dyer, W. D. Bates, P. Chen and T. J. Meyer, Application of Time-Resolved, Step-Scan Fourier Transform Infrared Spectroscopy to Excited-State Electronic Structure in Polypyridyl Complexes of Rhenium(I), *Inorg.*

- Chem.*, 1996, **35**, 273-274. (b) L. C. Abbott, C. J. Arnold, T.-Q. Ye, K. C. Gordon, R. N. Perutz, R. E. Hester and J. N. Moore, Ultrafast Time-Resolved UV-visible and Infrared Absorption Spectroscopy of Binuclear Rhenium(I) Polypyridyl Complexes in Solution, *J. Phys. Chem. A*, 1998, **102**, 1252-1260. (c) D. M. Dattelbaum, K. M. Omberg, J. R. Schoonover, R. L. Martin and T. J. Meyer, Application of Time-Resolved Infrared Spectroscopy to Electronic Structure in Metal-To-Ligand Charge-Transfer Excited States, *Inorg. Chem.*, 2002, **41**, 6071-6079. (d) A. Gabrielsson, P. Matousek, M. Towrie, F. Hartl, S. Zalis and A. Vlcek, Excited States of Nitro-Polypyridine Metal Complexes and Their Ultrafast Decay. Time-Resolved IR Absorption, Spectroelectrochemistry, and TD-DFT Calculations of fac-[Re(Cl)(CO)₃(5-nitro-1,10-phenanthroline)]. *J. Phys. Chem. A*, 2005, **109**, 6147-6153.
- (5) (a) V. Balzani, P. Ceroni and A. Juris, *Photochemistry and Photophysics. Concepts, Research, Applications*, Wiley-VCH, Weinheim: 2014. (b) M. Chergui, On the Interplay between Charge, Spin and Structural Dynamics In Transition Metal Complexes, *Dalton Trans.*, 2012, **41**, 13022-13029. (c) A. M. Blanco-Rodriguez, H. Kvapilova, J. Sykora, M. Towrie, C. Nervi, G. Volpi, S. Zalis and A. Vlcek, Photophysics of Singlet and Triplet Intraligand Excited States in [ReCl(CO)₃(1-(2-pyridyl)-imidazo[1,5- α]pyridine)] Complexes, *J. Am. Chem. Soc.*, 2014, **136**, 5963-5973.
- (6) (a) D. Donghi, G. D'Alfonso, M. Mauro, M. Panigati, P. Mercandelli, A. Sironi, P. Mussini and L. D'Alfonso, A New Class of Luminescent Tricarbonyl Rhenium(I) Complexes Containing Bridging 1,2-Diazine Ligands: Electrochemical, Photophysical, and Computational Characterization, *Inorg. Chem.*, 2008, **28**, 4243-4255. (b) M. Panigati, M. Mauro, D. Donghi, P. Mercandelli, P. Mussini, L. De Cola and G. D'Alfonso, Luminescent dinuclear rhenium(I) complexes containing bridging 1,2-diazine ligands: Photophysical properties and application, *Coord. Chem. Rev.*, 2012, **256**, 1621-1643.
- (7) M. Mauro, M.; E. Quartapelle Procopio, Y. Sun, C. H. Chien, D. Donghi, M. Panigati, P. Mercandelli, P. Mussini, G. D'Alfonso and L. De Cola, Highly Emitting Neutral Dinuclear Rhenium Complexes as Phosphorescent Dopants for Electroluminescent Devices, *Adv. Funct. Mater.*, 2009, **19**, 2607-2614.

- (8) (a) E. Quartapelle Procopio, M. Mauro, M. Panigati, D. Donghi, P. Mercandelli, A. Sironi, G. D'Alfonso and L. De Cola, Highly Emitting Concomitant Polymorphic Crystals of a Dinuclear Rhenium Complex, *J. Am. Chem. Soc.*, 2010, **132**, 14397-14399. (b) M. Mauro, C.-H. Yang, C.-Y. Shin, M. Panigati, C.-H. Chang, G. D'Alfonso and L. De Cola, Phosphorescent Organic Light-Emitting Diodes with Outstanding External Quantum Efficiency using Dinuclear Rhenium Complexes as Dopants, *Adv. Mater.*, 2012, **24**, 2054–2058.
- (9) (a) E. Ferri, D. Donghi, M. Panigati, G. Prencipe, L. D'Alfonso, I. Zanoni, C. Baldoli, S. Maiorana, G. D'Alfonso and E. Licandro, Luminescent conjugates between dinuclear rhenium(I) complexes and peptide nucleic acids (PNA) for cell imaging and DNA targeting, *Chem. Commun.*, 2010, **46**, 6255-6257. (b) C. Mari, M. Panigati, L. D'Alfonso, I. Zanoni, D. Donghi, L. Sironi, M. Collini, S. Maiorana, C. Baldoli, G. D'Alfonso and E. Licandro, Luminescent Conjugates between Dinuclear Rhenium Complexes and Peptide Nucleic Acids (PNA): Synthesis, Photophysical Characterization, and Cell Uptake, *Organometallics*, 2012, **31**, 5918-5928.
- (10) G. Valenti, M. Panigati, A. Boni, G. D'Alfonso, F. Paolucci and L. Prodi, Diazine bridged dinuclear rhenium complex: New molecular material for the CO₂ conversion, *Inorg. Chim. Acta*, 2014, **417**, 270-273.
- (11) D. M. Guldi, M. Maggini, E. Menna, G. Scorrano, P. Ceroni, M. Marcaccio, F. Paolucci and S. Roffia, A Photosensitizer Dinuclear Ruthenium Complex: Intramolecular Energy Transfer to a Covalently Linked Fullerene Acceptor, *Chem. Eur. J.*, 2001, **7**, 1597-1605.
- (12)(a) C. Luo, M. Fujitsuka, A. Watanabe, O. Ito, L. Gan, Y. Huang and C. H. Huang, Substituent and Solvent Effects on Photoexcited States of Functionalized Fullerene[60], *J. Chem. Soc., Faraday Trans.*, 1998, **94**, 527-532. (b) M. Prato and M. Maggini, Fulleropyrrolidines: a Family of Full-Fledged Fullerene Derivatives. *Acc. Chem. Res.* 1998, **31**, 519-526.
- (13) B. Albinsson and J. Martensson, Long-Range Electron and Excitation Energy Transfer in Donor–Bridge–Acceptor Systems, *J. Photochem. Photobiol., C*, 2008, **9**, 138-155, and references therein.

- (14)(a) A. Cannizzo, A. M. Blanco-Rodriguez, A. El Nahhas, J. Sebera, S. Zalis, A. Vlcek and M. Chergui, Femtosecond Fluorescence and Intersystem Crossing in Rhenium(I) Carbonyl-Bipyridine Complexes, *J. Am. Chem. Soc.*, 2008, **130**, 8967-8974. (b) A. El Nahhas, C. Consani, A. M. Blanco-Rodriguez, K. M. Lancaster, O. Braem, A. Cannizzo, M. Towrie, I. Clark, S. Zalis, M. Chergui and A. Vlcek, Ultrafast Excited-State Dynamics of Rhenium(I) Photosensitizers $[\text{Re}(\text{Cl})(\text{CO})_3(\text{N},\text{N})]$ and $[\text{Re}(\text{imidazole})(\text{CO})_3(\text{N},\text{N})]^+$: Diimine Effects, *Inorg. Chem.*, 2011, **50**, 2932-2943.
- (15)(a) J. P. Mittal, Excited States and Electron Transfer Reactions of Fullerenes, *Pure Appl. Chem.*, 1995, **67**, 103-110. (b) D. M. Guldi, G. Torres-Garcia and J. Mattay, Intramolecular Energy Transfer in Fullerene Pyrazine Dyads, *J. Phys. Chem. A*, 1998, **102**, 9679-9685. (c) A. Kahnt, J. Karnbratt, L. J. Esdaile, M. Hutin, K. Sawada, H. L. Anderson and B. Albinsson, Temperature Dependence of Charge Separation and Charge Recombination in Porphyrin Oligomer-Fullerene Donor-Acceptor Systems, *J. Am. Chem. Soc.*, 2011, **133**, 9863-9871. (d) K. M. Kaunisto, P. Vivo, R. K. Dubey, V. I. Chukharev, A. Efimov, N. V. Tkachenko and H. J. Lemmetyinen, Charge-Transfer Dynamics in Poly(3-hexylthiophene):Perylenediimide- C_{60} Blend Films Studied by Ultrafast Transient Absorption, *J. Phys. Chem. C*, 2014, **118**, 10625-10630.
- (16) For spectroelectrochemistry of other substituted fullerenes, see: L. Kavan and L. Dunsch, Spectroelectrochemistry of Carbon Nanostructures, *ChemPhysChem*, 2007, **14**, 974-998.
- (17) M. Maggini, D. M. Guldi, S. Mondini, G. Scorrano, F. Paolucci, P. Ceroni and S. Roffia, Photoinduced Electron Transfer in a Tris(2,2'-bipyridine)- C_{60} -Ruthenium(II) Dyad: Evidence of Charge Recombination to a Fullerene Excited State, *Chem. Eur. J.*, 1998, **4**, 1992-2000.
- (18) D. Armpach, E. C. Constable, F. Diederich, C. E. Housecroft and J.-F. Nierengarten, Bucky Ligands: Synthesis, Ruthenium(II) Complexes, and Electrochemical Properties, *Chem. Eur. J.*, 1998, **4**, 723-733.
- (19) F. Nastasi, F. Puntoriero, S. Campagna, S. Schergna, M. Maggini, F. Cardinali, B. Delavaux-Nicot and J.-F. Nierengarten, A Luminescent Multicomponent Species Made of Fullerene and Ir(III) Cyclometallated Subunits, *Chem. Comm.*, 2007, 3557-3558.

- (20) F. Cardinali, H. Mamlouk, Y. Rio, N. Armaroli and J.-F. Nierengarten, Fullerohelicates: A New Class of Fullerene-containing Supermolecules, *Chem. Comm.*, 2004, 1582-1583.
- (21) N. Armaroli, G. Accorsi, D. Felder and J.-F. Nierengarten, Photophysical Properties of the Re(I) and Ru(II) Complexes of a New C₆₀-Substituted Bipyridine Ligand, *Chem. Eur. J.*, 2002, **8**, 2314-2322.

Supporting information to:

Photoinduced intercomponent excited-state decays in a molecular dyad made of a dinuclear rhenium(I) chromophore and a fullerene electron acceptor unit

Francesco Nastasi,^a Fausto Puntoriero,^a Mirco Natali,^b Miriam Mba,^c Michele Maggini,*^c Patrizia Mussini,^d Monica Panigati,*^{d,e} and Sebastiano Campagna.*^{a,f}*

(a) Dipartimento di Scienze Chimiche, Università di Messina and Centro Interuniversitario per la Conversione Chimica dell'Energia Solare (SOLAR-CHEM; sezione di Messina), Messina, Italy. (b) Dipartimento di Scienze Chimica e Farmaceutiche, Università di Ferrara and Centro Interuniversitario per la Conversione Chimica dell'Energia Solare (SOLAR-CHEM; sezione di Ferrara), Ferrara, Italy. (c) Dipartimento di Scienze Chimiche, Università di Padova, Padova, Italy. (d) Dipartimento di Chimica, Università degli Studi di Milano, Milano, Italy. (e) Istituto per lo Studio delle Macromolecole (ISMAL)-CNR, Milano, Italy. (f) Istituto per la Sintesi Organica e la Fotoreattività (ISOFO)-CNR, Bologna, Italy.

INDEX

Materials, equipments, and methods (including information on the synthesis of 2 and 3)	page S2
Calculation of Förster rate constant for energy transfer process	page S4
Synthesis	page S5
Scheme S1: Schematic synthesis of 1	page S5
Synthesis of ligand 6 .	page S5
Synthesis of fullerene ligand 7	page S6
Synthesis of the dyad 1	page S6
Comments on the possible presence of diastereoisomers in 1	page S7
Figure S1: Time-dependent recovery of the MLLCT bleaching at 400 nm of 2	page S8
Figure S2: Transient absorption rise and decay of 1 at 680 nm	page S8
Figure S3: NIR transient spectra of 2 .	page S9
Figure S4: Spectroelectrochemistry of 3 .	page S9
Figure S5: Global kinetic analysis of the time-resolved transient absorption spectra of 1	
Comments on the global kinetic analysis of 1	page S10
References:	page S11

Materials, equipments, and methods

All reagents were obtained from commercial suppliers and used without further purification; where needed, solvents were deoxygenated and dried by standard methods. 4-(Pyridazin-4-yl)-butanoic acid, complex **2** and fulleropyrrolidine **3** were prepared according to literature procedures.¹ [60]Fullerene was purchased from Bucky-USA. All reactions involving the rhenium complexes were performed using the Schlenk technique. Flash-chromatography was performed over SiO₂ (Macherey-Nagel 60 M, 0.04-0.063 μm, 230-400 mesh for derivatives **3-5**; 70-230 mesh for dyad **1**). ¹H and ¹³C NMR spectra were recorded at 301 K on a Bruker AC-300, AC-500 or AC-250 instruments using the partially deuterated solvent as the internal reference. The multiplicity of a signal is indicated as: br - broad, s - singlet, d - doublet, t - triplet, q - quartet, m - multiplet, dd - doublet of doublets, dt - doublet of triplets, etc. FT-IR absorption spectra were recorded with a Nicolet 5700 FT-IR spectrophotometer or on a Bruker Vector22 FT instrument. Atmospheric pressure photoionization mass spectroscopy (APPI-MS) was performed in a ESI-TOF Mariner™ Biospectrometry™ Workstation of Applied Biosystems by direct infusion of a cyclohexane solution. Preparative HPLC was performed on a Shimadzu LC-8A equipped with a UV detector at 340 nm and a Buckyprep column, using toluene as eluent at a rate of 8mL/min. UV/Vis absorption spectra were recorded with a Jasco V-560 and Varian Cary 5000 and Cary 100 spectrophotometers. For steady-state luminescence measurements, a Jobin Yvon-Spex Fluoromax P spectrofluorimeter was used, equipped with a Hamamatsu R3896 photomultiplier. The spectra were corrected for photomultiplier response using a program purchased with the fluorimeter. For the luminescence lifetimes, an Edinburgh OB 900 time-correlated single-photon-counting spectrometer was used. A Hamamatsu PLP 2 laser diode (59 ps pulse width at 408 nm) and/or nitrogen discharge (pulse width 2 ns at 337 nm) were employed as excitation sources. Emission quantum yields for deaerated solutions were determined by the optically diluted method² with [Ru(bpy)₃]²⁺ (bpy = 2,2'-bipyridine) in air equilibrated aqueous solution as quantum yield standard ($\Phi_{em} = 0.028$).³

Time-resolved transient absorption experiments were performed using a pump-probe setup based on the Spectra-Physics MAI-TAI Ti:sapphire system as the laser source and the Ultrafast Systems Helios spectrometer as the detector. The pump pulse was generated using a Spectra-Physics 800 FP OPA instrument. The probe pulse was obtained by continuum generation on a sapphire plate (spectral range 450–800 nm). The effective time resolution was around 200 fs, and the temporal chirp over the white-light 450–750 nm range around 150 fs; the temporal window of the optical delay stage was 0–3200 ps. NIR extension to the multichannel pump-probe transient absorption spectrometer was used for the near-infrared experiments. A fiber optics coupled multichannel spectrometer with InGaAs sensor have been used as NIR detector. The extension allows for probing

the photoinduced transients in the 800-1600 nm range, with 3.5 nm intrinsic resolution (sensitivity range: 800-1600 nm; maximum spectral acquisition rate- 7900 spectra/s). In order to cancel out orientation effects on the dynamics, the polarization direction of the linearly polarized probe pulse was set at a magic angle of 54.7° with respect to that of the pump pulse. Please note that all the transient spectra shown in the present paper are chirp corrected. The chirp correction was done by using the pump induced absorption signals themselves in the same conditions (same cuvette, solvent, temperature, stirring frequency...) used for each single experiment. All the time-resolved data were analyzed with the Ultrafast Systems Surface Explorer Pro software.⁴

Nanosecond transient absorption measurements were performed with an Applied Photophysics laser flash photolysis apparatus, using a frequency-tripled (355 nm, 160 mJ) Surelite Continuum II Nd/YAG laser pulse (half-width 6-8 ns) as excitation source and a 150 W Xenon arc-lamp as probe light. Transient detection was obtained using a photomultiplier-oscilloscope combination (Hamamatsu R928, LeCroy 9360).

Electrochemical measurements were carried out in argon purged 1,2-dichloroethane at room temperature with an Autolab multipurpose equipment interfaced to a PC. The working electrode was a glassy carbon (8 mm^2 , Amel) electrode. The counter electrode was a Pt wire, and the reference electrode was an SCE separated with a fine glass frit. The concentration of the complexes was about 5×10^{-4} M. Tetrabutylammonium hexafluorophosphate was used as a supporting electrolyte and its concentration was 0.05 M. Differential pulse voltammetry (DPV) was obtained at scan rates of 4, 10, 20 mV s^{-1} . Redox potentials were corrected by the internal reference ferrocene (395 mV vs. SCE).

UV-vis-NIR spectroelectrochemical measurements were obtained with a SPECAC Omni Cell System: an optically transparent thin-layer electrode (OTTLE) cell with the working Pt-mesh, twinned Ag-wire reference and Pt-mesh auxiliary electrodes melt-sealed into a polyethylene spacer – CaF_2 windows and 0.25 mm path length. The UV-vis-NIR spectra were registered with a JASCO V570 spectrophotometer concurrently applying a potential by using an Autolab multipurpose equipment interfaced to a PC. TBAPF_6 , (+99%) supporting electrolyte and toluene solvent (anhydrous, 99.8%) were supplied by Aldrich.

Experimental uncertainties are as follows: absorption maxima, 2 nm; molar absorption, 15%; luminescence maxima, 4 nm; luminescence lifetimes, 10%; luminescence quantum yields, 15%; transient absorption decay and rise rates, 10%; redox potentials, 15 mV.

Förster rate constant for energy transfer process

Assuming Förster energy transfer as the leading mechanism, the rate constant can be calculated by the simplified equation S1.

$$k_{en}^F = 8.8 \times 10^{-25} \frac{K^2 \Phi}{n^4 r_{AB}^6 \tau} J_F \quad (S1)$$

In this equation, k_{en}^F is the rate constant of the energy transfer process, K is an orientation factor which accounts for the directional nature of the dipole-dipole interaction, Φ and τ are the luminescence quantum yield and lifetime of the donor model, respectively, n is the solvent refractive index, r_{AB} is the distance (in Å) between donor and acceptor. Considering the subunits of the species as freely rotating along the bond axis, the random value for the orientation factor (0.667) was assumed.

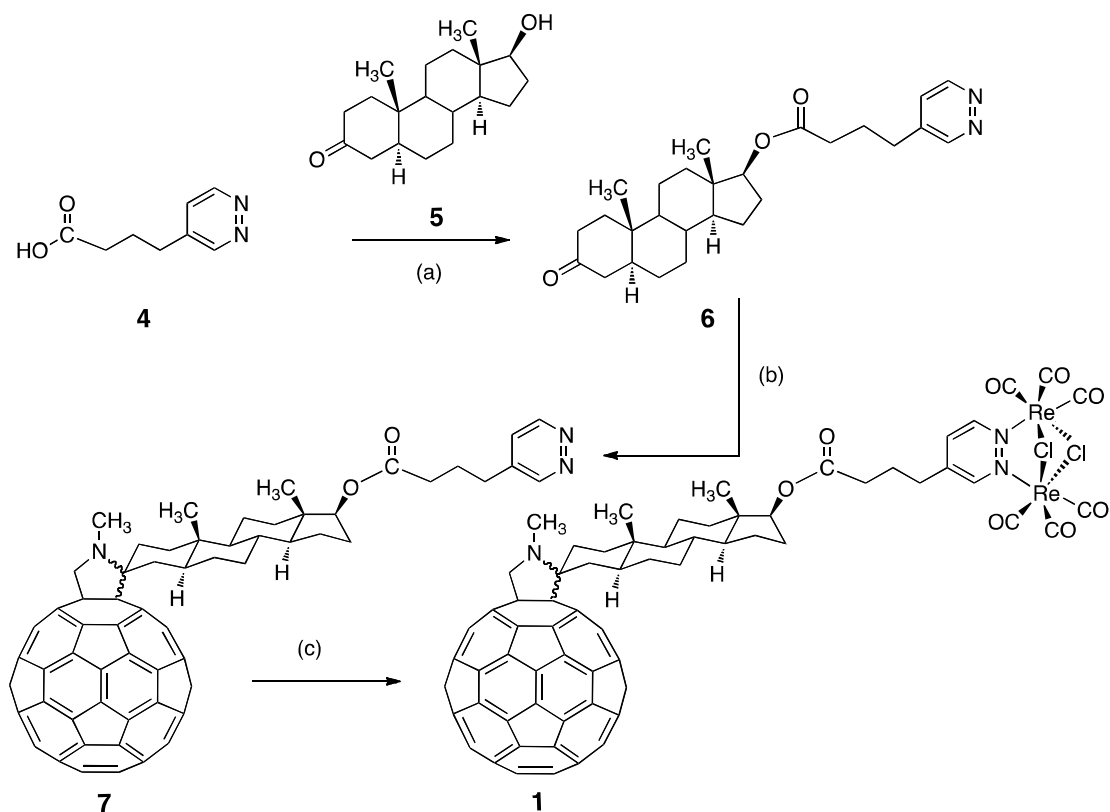
The overlap integral J_F for Förster interaction can be calculated according to equation S2.

$$J_F = \frac{\int F(\bar{\nu}) \varepsilon(\bar{\nu}) / \bar{\nu}^4 d\bar{\nu}}{\int F(\bar{\nu}) d\bar{\nu}} \quad (S2)$$

In this equation, $F(\bar{\nu})$ is the luminescence spectrum of the donor model, and $\varepsilon(\bar{\nu})$ is the absorption spectrum of the acceptor on an energy scale (cm^{-1}).

This equation has been applied to calculate the energy transfer from the dirhenium chromophore to the fullerene subunit in **1**. The relevant spectroscopic and photophysical data were derived from the model species **2** and **3**. The orientation factor was assumed to be 2/3, the statistical value allowing free rotation. The donor-acceptor distance was assumed to be 10 Å, a quite, probably extreme, compact conformation (note that the dimension of the steroid moiety is 11 Å). With such approximations, time constant for the dirhenium-to-fullerene energy transfer according to the Förster mechanism in **1** is 13 ns, much slower than the experimental value of the quenching of dirhenium-based MMLCT excited state (about 100 ps, see main text).

Synthesis



Scheme S1. Synthesis of dyad **1**. Reagents and conditions : (a) DCC/DMAP, CH₂Cl₂, 24h, 38%; (b) N- methylglycine, C₆₀, toluene, reflux, 4h, 10%; (c) [ReCl(CO)₅], toluene, reflux, 3 h, 70 %

Synthesis of ligand 6. N,N'-dicyclohexylcarbodiimide (DCC) (69 mg, 0.36 mmol), 4-(dimethylamino)pyridine (DMAP) (66 mg, 0.54 mmol) and 5 α -androstan-17 β -ol-3-one (84 mg, 0.29 mmol) were added in this order to a solution of 4-(pyridazine-4-yl)butanoic acid **4** (40 mg, 0.24 mmol) in CH₂Cl₂ (5 mL). The mixture was stirred at room temperature for 24 h, then water was added, the layers were separated and the organic phase was washed with NaHCO₃ 5% (3 \times 15 mL), brine (3 \times 15mL) and dried over Na₂SO₄. The solvent was evaporated under reduced pressure and the residue was purified by flash chromatography (silica gel, toluene/AcOEt 6:4) affording 40 mg (38%) of **6** as a yellowish solid.

¹H NMR (300 MHz, CDCl₃) δ : 9.01 (m, 2H), 7.27 (m, 1H), 4.54 (t, 1H, $J = 7.2$ Hz), 2.63 (t, 2H, $J = 7.5$ Hz), 2.35-0.67 (m, 23H), 2.30 (t, 2H, $J = 7.2$ Hz), 2.03-1.80 (m, 2H), 0.95 (s, 3H), 0.73 (s, 3H). ¹³C NMR (75 MHz, CDCl₃) δ : 211.7, 172.52, 152.60, 150.96, 140.62, 125.80, 82.85, 53.57, 50.41, 46.48, 44.51, 42.58, 38.36, 37.98, 36.78, 35.59, 35.03, 33.12, 31.64, 31.07, 28.61, 27.46, 24.71, 23.40, 20.78, 11.13, 11.35 ppm. ESI-MS (CH₃CN+0.1% HCOOH) m/z : [M+H]⁺ calcd. for

(C₂₇H₃₉N₂O₃⁺) 438.6; found 439.5 [M+H]. IR (KBr) ν : 3429, 3046, 2972, 2933, 2850, 1721, 1444, 1388, 1369, 1358, 1331, 1297, 1172, 1142, 1048, 1007, 979, 956, 879, 764, 730, 701 cm⁻¹.

Synthesis of fullerene ligand 7. Compound **6** (40 mg, 0.1 mmol) was added to a solution of [60]fullerene (55 mg, 0.08 mmol) and N-methylglycine (81 mg, 0.8 mmol) in toluene (56 mL). The mixture was heated to reflux temperature until complete consumption of **6** (TLC, toluene/AcOEt 6:4). The mixture was then cooled to room temperature, evaporated to dryness and the residue was purified by flash chromatography (silica gel, toluene/AcOEt 9:1, then 6:4). The resulting solid was dissolved in the minimum amount of toluene, precipitated from methanol and centrifuged, affording 11 mg (10%) of ligand **7** as a brown solid.

¹H NMR (250 MHz, CS₂/CDCl₃ 9:1) δ : 9.13-9.00 (m, 2H), 7.32-7.27 (m, 1H), 5.14-4.93 (m, 2H), 4.73-4.59 (m, 1H), 3.52 (s, 3H), 2.96 (s), 2.78-0.62 (m, 34H) ppm. ¹³C NMR (63 MHz, CS₂/CDCl₃ 9:1) δ : 180.67, 163.26, 163.17, 161.01, 159.38, 155.29, 155.16, 154.93, 154.78, 154.70, 154.51, 154.47, , 154.45, 154.31, 154.29, 154.27, 153.89, 153.75, 153.71, 153.68, 153.62, 153.59, 153.56, 153.45, 152.97, 152.89, 152.85, 152.83, 151.72, 151.18, 151.13, 151.11, 151.09, 151.08, 150.80, 150.80, 150.71, 150.67, 150.66, 150.60, 150.41, 150.38, 150.34, 150.29, 150.25, 150.00, 148.91, 148.77, 148.72, 148.44, 148.38, 143.89, 143.82, 134.06, 92.36, 91.56, 88.36, 87.07, 84.65, 80.54, 77.91, 63.11, 63.06, 59.50, 51.77, 51.34, 51.15, 47.31, 45.79, 44.98, 44.37, 44.22, 43.93, 41.92, 41.86, 40.47, 40.43, 37.42, 36.34, 33.70, 32.29, 29.34, 20.97, 20.94, 9.55 ppm. APPI-MS (negative mode, cyclohexane) m/z : calcd. for C₈₉H₄₃N₃O₂ 1185, found 1185, 720 (C₆₀). UV-Vis (cyclohexane) λ : 431.5, 417.5, 318.5, 256.0, 231.0 nm.

Synthesis of the dyad 1. To a solution of [ReCl(CO)₅] (3.5 mg, 9.67 μ mol) in freshly distilled toluene (4 ml) in a Schlenk tube, fullerene ligand **7** (5.6 mg, 4.73 μ mol) was added and the mixture was refluxed for 3 h. The progress of the reaction was monitored by IR spectroscopy, following the disappearance of ν_{CO} of [ReCl(CO)₅] at 2046 (s), 1985 (m) cm⁻¹. The solution was evaporated to dryness under reduced pressure and the residue, dissolved in CH₂Cl₂, was precipitated with *n*-hexane affording a microcrystalline powder that was purified by column chromatography (SiO₂, CH₂Cl₂). Dyad **1** (6.0 mg, 70%) was isolated upon addition of *n*-hexane to a concentrated CH₂Cl₂ solution as a brownish microcrystalline powder. Anal. Calcd for Re₂C₉₅H₄₃O₈N₂Cl₂: C, 63.47; H, 2.41; N, 2.34. Found: C, 63.71; H, 2.57; N, 2.28. IR (CH₂Cl₂) ν_{CO} : 2050 (mw), 2033 (s), 1947 (s), 1917 (s), cm⁻¹. These IR signals are characteristics of dinuclear Re complexes having idealized C_{2v} symmetry and containing bridging nitrogen ligands and chlorides as ancillary ligands.^{1c} ¹H NMR (400 MHz, CD₂Cl₂): δ : 1.9-0.8 (m, 28H) 2.15 (q, 2H, H_b); 2.53 (t, 2H, H_c); 3.01 (t, 2H, H_a); 4.75 (t, 1H), 7.91-7.93 (dd, 1H, H₅); 9.64-9.69 (m, 2H, H₃, H₆). The insolubility of dyad **1** hampered the

registration of a meaningful ^{13}C NMR spectrum. UV-Vis (toluene) λ : 325, 435 nm.

Comments on the possible presence of diastereoisomers in **1**

The use of a diastereoisomeric mixture of ligand **7** to bind Re(I) (see **Scheme S1**) may, in principle, influence properties such as the rates of energy or electron transfer, because diastereoisomers have different spatial orientations. In addition, the short alkyl chain that connects the androstane spacer to the pyridazine ligand moiety can generate a number of different conformations for each diastereoisomer that further complicate the assessment of the respective orientation of the donor and acceptor moieties in dyad **1**. One of us considered these structural issues in a previous paper (cited in reference no. 17 of the main paper, i.e.: M. Maggini, *et al.*, *Chem. Eur. J.*, 1998, **4**, 1992-2000), whose topic is closely related to that of the present work, and found that diastereoisomerically pure dyads, based on the same androstane spacer as dyad **1**, essentially behave like their diastereoisomeric mixture when separately tested in photophysical experiments. Therefore, whereas diastereoisomers mixture can be present in **1**, this circumstance is not important for the photophysical properties here studied. The situation resembles the negligible effect of the presence of chiral isomers for photoinduced electron and energy transfer processes involving multimetallic compounds based on octahedral Ru(II)-polypyridine compounds.⁵

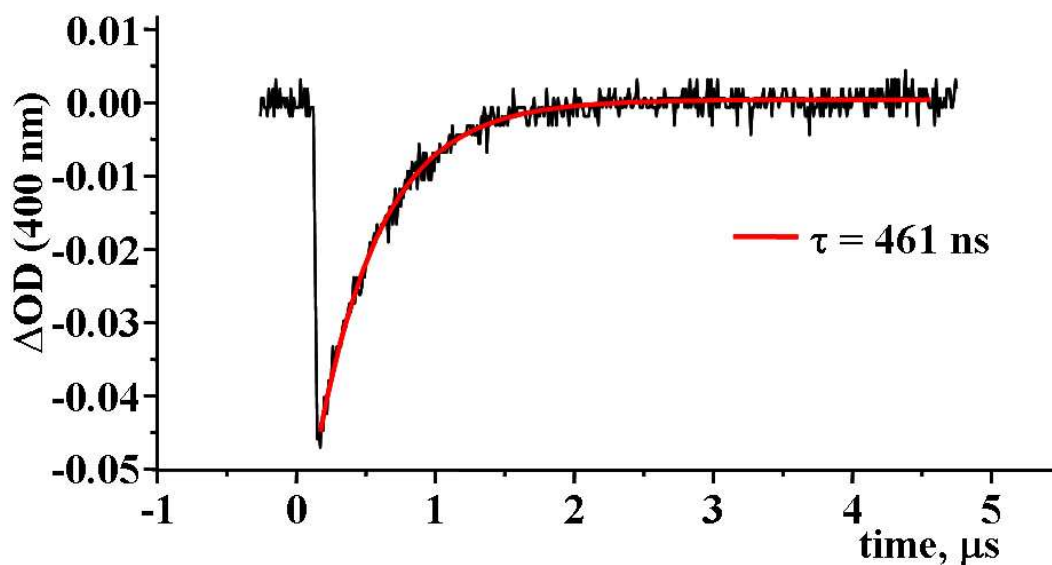


Figure S1. Time-dependent recovery of the MLLCT bleaching at 400 nm of **2** upon 355 nm excitation.

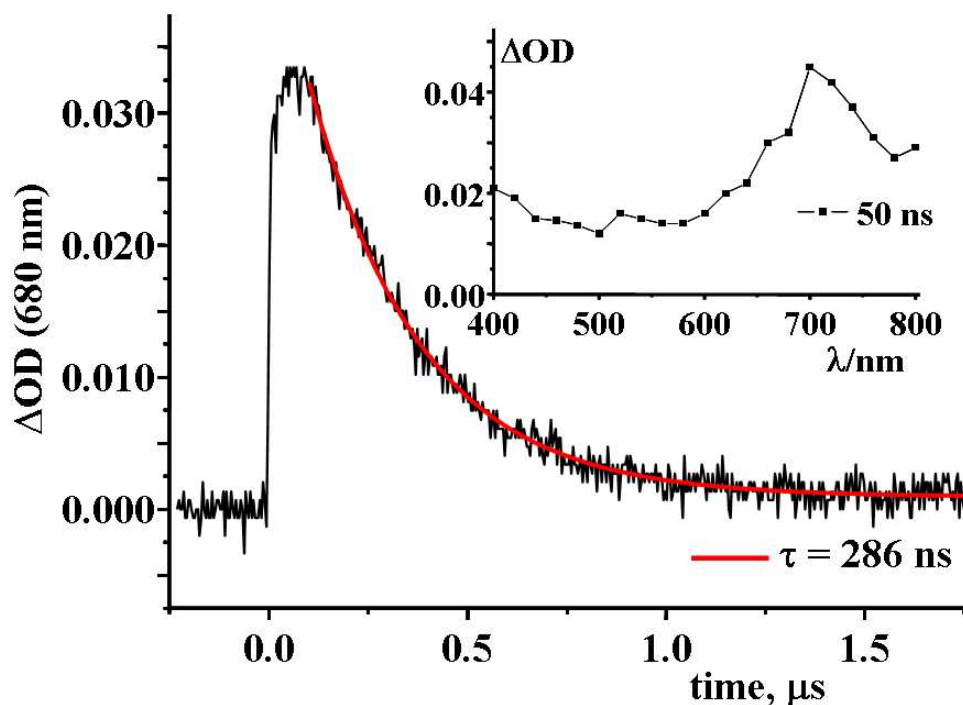


Figure S2. Transient absorption decay of **1** at 680 nm upon 355 nm excitation. For short delays after laser pulse a risetime is evidenced, which anyway is too fast to be calculated ($<10 \text{ ns}$). In the inset, the transient absorption spectrum of **1** after 50 ns from pulse is shown.

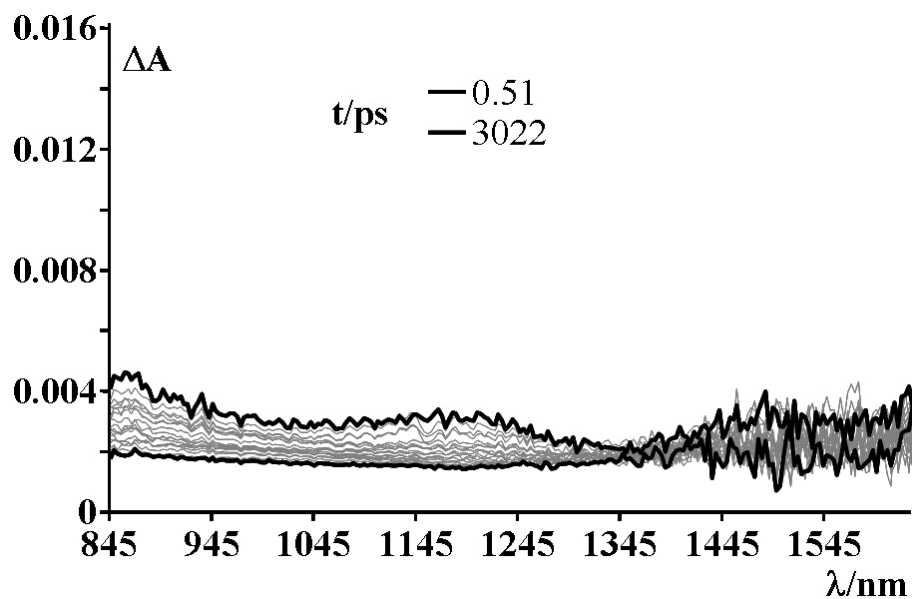


Figure S3. NIR transient spectra of **2**. No significant spectral feature is apparent.

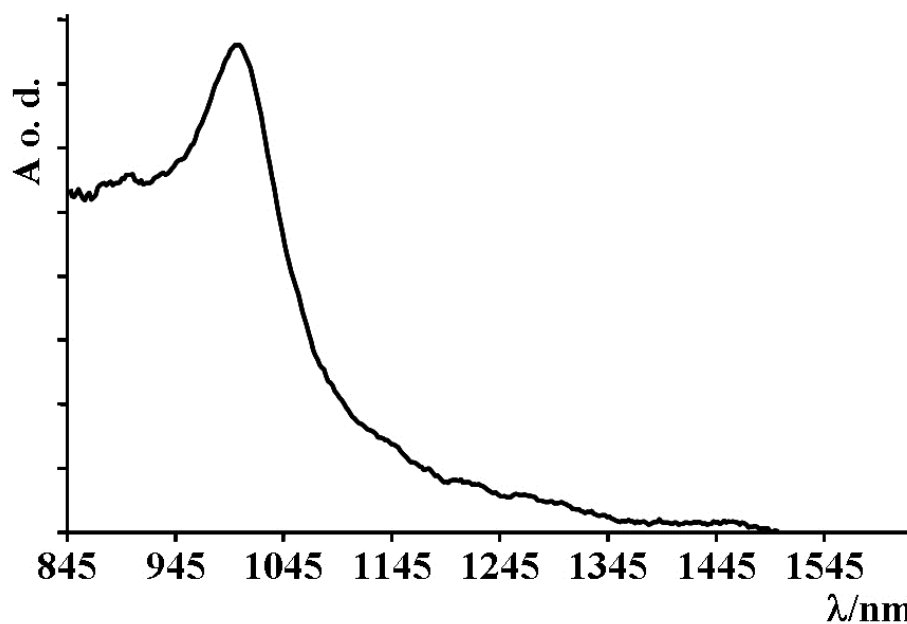


Figure S4. Spectroelectrochemistry of **3**. The spectrum is obtained by applying a potential of -0.85 V vs SCE at a solution of **3** in toluene. The peak maximum corresponds to the peak obtained in the spectra of Figure 6, top panel, attributed to the CS state.

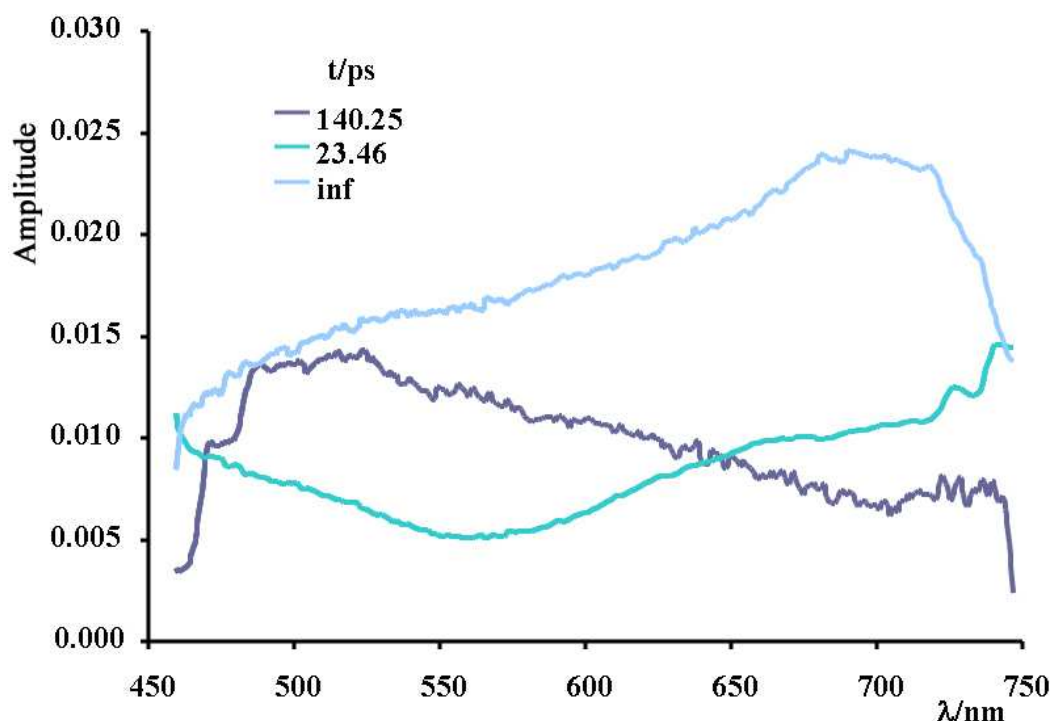


Figure S5. Spectral distributions of the pre-exponential amplitudes of the three lifetime components obtained for **1**, via global analysis on the singular value decomposition (SVD) of the principal spectral components of the transient absorption spectra. Comments in the text reported in ESI.

Comments on the global kinetic analysis of **1**

A global kinetic analysis was performed on the transient absorption spectra of **1** (see **Figure S5**). The analysis yields three reliable components. The shortest one (τ about 23 ps), which is similar to the initial transient spectrum shown in **Figure 5a**, fits the global time for vibrational cooling within the MLLCT triplet state of the metal center (two processes are calculated by single wavelength analysis for vibrational cooling, see **Figs. 5** and **6** in the main text, with 4 and 20 ps time constants; the shorter-lived process is not evidenced by global analysis); the second component (τ about 140 ps) agrees with the transient spectrum shown in **Figure 5b**, and is assigned to the charge-separated state (which is actually calculated to decay with a time constant of about 120 ps, see main text); the final spectrum, which has a decay time constant longer than the pump-probe experiment limit (3 ns), recalls the final spectrum in **Figure 5c**, and is assigned to the triplet state of the fullerene subunit (which indeed decays in the ns- μ s regime, see main text and **Figure S2**).

REFERENCES

- (1) (a) E. Ferri, D. Donghi, M. Panigati, G. Prencipe, L. D'Alfonso, I. Zanoni, C. Baldoli, S. Maiorana, G. D'Alfonso, E. Licandro, *Chem. Commun.* 2010, **46**, 6255. (b) D. M. Guldi, M. Maggini, E. Menna, G. Scorrano, P. Ceroni, M. Marcaccio, P. Paolucci, S. Roffia, *Chem. Eur. J.* 2001, **7**, 1597. (c) M. Panigati, M. Mauro, D. Donghi, P. Mercandelli, P. Mussini, L. De Cola, G. D'Alfonso, *Coord. Chem. Rev.* 2012, **256**, 1621.
- (2) J. N. Demas, G. A. Crosby, *J. Phys. Chem.*, 1971, **75**, 991.
- (3) K. Nakamaru, *Bull. Chem. Soc. Jpn.*, 1982, **55**, 2697.
- (4) <http://www.ultrafastsystems.com/surfexp.html>.
- (5) V. Balzani, S. Campagna, G. Denti, A. Juris, S. Serroni, M. Venturi, *Acc. Chem. Res.*, 1998, **31**, 26.